Journal of Power Sources 251 (2014) 137–144

Contents lists available at ScienceDirect

Journal of Power Sources

journal homepage: www.elsevier.com/locate/jpowsour

Experimental evaluation of the performance of the sodium metal chloride battery below usual operating temperatures

Eirini Gerovasili [a,*], Johanna F. May [a], Dirk Uwe Sauer [b]

[a] Robert Bosch GmbH, Robert-Bosch-Strasse 2, D-71701 Schwieberdingen, Germany
[b] Institut for Power Electronics and Electrical Drives (ISEA), RWTH Aachen University, Jaegerstrasse 17-19, D-52066 Aachen, Germany

HIGHLIGHTS

- A sodium–metal chloride battery was cycled at 240 °C and 260 °C.
- At 0.1C discharge rate the usable discharged energy was maximized at 240 °C.
- The duration of charging was measured for charging voltages up to 2.7 V/cell.
- At 240 °C the daily efficiency was higher compared to 275 °C.

ARTICLE INFO

Article history:
Received 13 September 2013
Received in revised form
28 October 2013
Accepted 9 November 2013
Available online 28 November 2013

Keywords:
ZEBRA battery
Sodium–metal chloride battery
Low temperature
Efficiency

ABSTRACT

The high operating temperature of the sodium metal chloride battery limits the possible applications of this storage technology. In this study, the performance of a 3.65 kWh (80 Ah, 48 V) battery at temperatures as low as 240 °C is measured and the efficiency at different discharge currents, cycling frequencies and operating temperatures is examined. The total available capacity of a 40 Ah string at 240 °C when discharging with 0.1C is found to be just 1 Ah smaller compared to 275 °C, which is the nominal operating temperature of the battery. However it is shown that low temperatures have a big impact on the charge duration. Starting from 20% SOC (state-of-charge) the duration of charging until the fulfillment of the end-of-charge criterion at 240 °C is 25 h with the quickest charging regime (0.25C, 2.7 V/cell) whereas until 90% SOC 7.6 h are required. At a limited SOC operation window from 20% to 90% the total daily efficiency of the 3.65 kWh battery is higher at 240 °C compared to 275 °C and increases from 69% if one cycle is performed daily with 0.175C discharge current to 81% for two cycles with the same discharge rate.

1. Introduction

The sodium metal chloride battery consists of a solid metal, sodium chloride cathode and a liquid sodium anode. The used metal can be exclusively nickel or a mixture of nickel and iron. A unique characteristic of the sodium metal chloride batteries compared to other battery chemistries is their solid β″-alumina ceramic electrolyte which allows the migration of Na-ions while acting as an electronic insulator [1].

During discharge the following reaction takes place in the positive electrode:

$$NiCl_2 + 2Na^+ + 2e^- \rightarrow Ni + 2NaCl \quad OCV \simeq 2.58\ V \tag{1}$$

whereas in the negative electrode Na-ions are generated:

$$Na \rightarrow Na^+ + e^-$$

If while discharging the voltage of each cell drops below 2.35 V/cell a second reaction starts in the cathode adjacent to the beta alumina tube:

$$FeCl_2 + 2Na^+ + 2e^- \rightarrow Fe + 2NaCl \quad OCV \simeq 2.35\ V \tag{2}$$

When both active materials are present and the voltage is below the 2.35 V/cell threshold the discharge voltage can be calculated by assuming a sodium metal chloride cell with only $NiCl_2$ in the cathode (Ni-cell) connected in parallel with a sodium iron chloride cell (Fe-cell). If the voltage rises again above that threshold, the Fe-cell is recharged by the available $NiCl_2$ according to:

* Corresponding author. Tel.: +49 (711)811 34508; fax: +49 (711)811 2853.
E-mail addresses: eirini.gerovasili@de.bosch.com, gerovasili@gmx.de (E. Gerovasili).

0378-7753/$ – see front matter
http://dx.doi.org/10.1016/j.jpowsour.2013.11.046

Table 1
Specifications of the tested battery.

Nominal voltage [V]	Nominal capacity[a] [Ah]	Nominal energy[a] [kWh]	Weight [kg]	Thermal conductivity of insulating material according to EN 12667 [$Wm^{-1} K^{-1}$]	Thickness of insulation [mm]	Dimensions of outer case [mm]	Nominal operating temperature [°C]
48	80	3.65	45	0.023[b]	~43	260 × 550 × 320	275 °C

[a] Measured with 0.25C until 42 V.
[b] At 200 °C.

$NiCl_2 + Fe \rightarrow Ni + FeCl_2$

Since the ionic conductivity of the beta alumina increases non-linearly with higher temperatures, an acceptable battery performance was reported for a temperature range of 270 °C–350 °C [2,3]. However, the lowest theoretical operation temperature is 157 °C [4]. This temperature is dictated by the melting point of the secondary liquid electrolyte, which facilitates the movement of the sodium ions in the positive electrode. In order to maintain an appropriate operating temperature, the battery features internal heaters and it is enclosed in a thermally insulated battery case that reduces the heat dissipation [2]. If the stored energy is used for powering the internal heating system, the self-discharge of the battery in stand-by mode was reported to be 10–15%/day for a battery featuring vacuum insulation [2,5]. Even though the heat losses are partially compensated by the Joule heat generated in the internal resistance during operation, the heating demand of the sodium metal chloride battery worsens the overall efficiency, especially in low-current application. Until recently, research has focused on the use of the high-temperature sodium metal chloride battery as back-up power source in telecommunication applications [6,7] and in electric vehicles [8–10] with an operating internal temperature above 270 °C. Much lower temperatures that would reduce significantly the heat transfer losses have been tested in planar-type sodium nickel chloride cells. In these cells the degradation at temperatures as low as 175 °C after 60 cycles was examined [11]. The total cell polarization was found to increase quicker at 280 °C due to the growth of the grain size of nickel and sodium chloride in the cathode whereas it remained almost constant at 175 °C. Promising results regarding the anticipated lifetime at lower than the usual temperature range have been delivered by the common tubular cells as well. In Ref. [12] an accelerated lifetime test with ML3-X type cells, charged with 3.1 V/cell, showed that the cell resistance at the end of charge after 300 cycles was below 80 mΩ at 260 °C whereas at 350 °C it exceeded that value.

Goal of the present study is to figure out the feasibility of low-temperature operation, quantify the possible benefits and identify the limitations. For this purpose, a detailed analysis of the

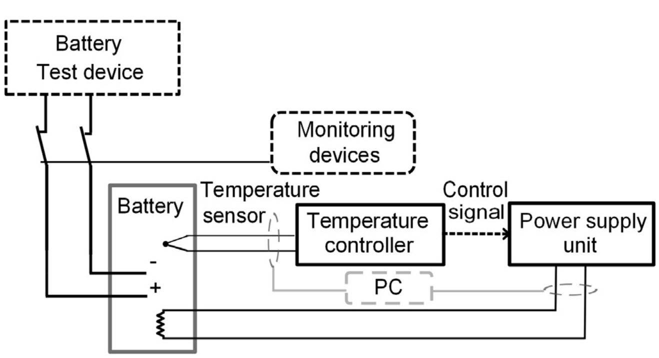

Fig. 1. Sketch of the test bench used for the measurements.

electrochemical performance of a sodium metal chloride battery with tubular cells at 240 °C, 260 °C, 275 °C and 310 °C was made. Additionally, the heating demand in stand-by mode and in operation was measured.

2. Experimental setup

The 48TL80 battery from FIAMM-SoNick with the specifications shown in Table 1 was used for the measurements. It consists of ML3-X type cells with 40 Ah nominal capacity, which are connected in two parallel strings, each one with 20 cells in series. In these cells almost 76% of the nominal capacity derives from the Ni-cell. Microporous silica panels which are not evacuated are used as thermal insulation in this type of battery. The BMS (Battery Management System) delivered with the battery was set out of operation. Instead, a temperature controller was used for regulating the power unit that heated the battery with maximum 130 W. A sketch of the test bench is shown in Fig. 1. The required power for heating was provided externally and recorded continuously. No cooling measure was implemented. The room temperature remained constant at 21 °C throughout the measurements. Thermocouples installed near the center of the cell pack measured the internal temperature, which served as input for the temperature controller. The measured values of the temperature showed an oscillation of ±3 °C in stand-by mode. Thus a moving average filter with 100 s time constant was applied before the temperature was recorded. It should be noted here that the temperature difference between the cells in the middle of the battery case and the outer cells can be 10–15 °C.

The charge/discharge regimes were programmed and executed with a BaSyTec HPS battery tester (Basytec GmbH, Germany) which was connected to the battery strings and measured the relevant operating parameters with ±0.5% accuracy. For all the measurements a typical for the sodium metal chloride batteries IU-charge is used [2,13]: a charging current is imposed and the battery voltage starts rising. This is the constant current (CC) phase of the charge. Once the battery voltage reaches the charging voltage the constant voltage (CV) phase of the charging starts, in which the voltage is stable while the current decreases until the end-of-charge criterion of <1.25 mA Ah^{-1} for 0.5 h is met. The SOC (state-of-charge) was calculated based on an Ah-balance and on the nominal capacity of the battery.

3. Results and discussion

3.1. Open-circuit voltage (OCV) and DC-resistance at 240 °C

The OCV of the sodium metal chloride battery was measured at 240 °C (Fig. 2) after interrupting the charge and discharge process. The duration of the pauses varied from 6 h to 25 h depending on the stabilization tendency of the OCV. While discharging with 0.0625C constant current, the 2.35 V/cell threshold is reached at 24% SOC. At this point the Fe-reaction starts next to the beta-alumina separator. During the next pause at 20% SOC, the Fe-cell is gradually recharged

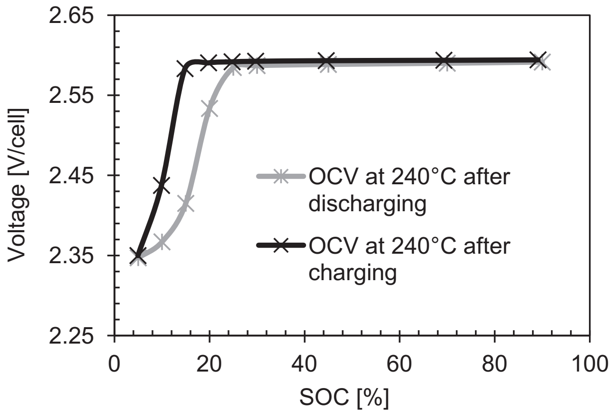

Fig. 2. OCV of a sodium metal chloride battery at 240 °C after at least 6 h pause. A hysteresis of the open circuit potential is observed between 5% and 25% SOC, i.e. the OCV does not depend only on the SOC but also on the history of charging, discharging.

from the remaining $NiCl_2$ and the final OCV of the battery, measured after 25 h, is higher than the OCV of the Fe-cell alone due to the contribution of the Ni-cell. At 15% SOC the final OCV is reached after 15 h. At this stage there is only little remaining $NiCl_2$ and the recharging process does not boost the OCV substantially. The theoretical OCV of the Fe-cell is measured at 5% SOC.

It is known that the internal resistance of the sodium metal chloride battery depends on the history of operation [10]. The measurement of the OCV after charging and after discharging at the same SOC reveals that this is also true for the OCV. Even if a coulombic efficiency of 99% is taken into account a hysteresis is observed from 5% to 25% SOC (Fig. 2). This phenomenon could be caused by the iron doping of the Ni-cell. When the charging of the battery begins the SOC of the Ni-cell and of the Fe-cell increase at the same time. On the contrary, when discharging with small currents, the Fe-cell remains fully charged until most of the nickel chloride is used up before it starts discharging. The difference in the SOC between the two partial cells after charging and after discharging even if the SOC of the battery is the same would result in different contribution of each one of them in the mixed OCV and thus to an OCV dependency on the history of the battery's use.

Based on the measured OCV the cell-resistance of the battery was calculated from Eq. (3) while discharging continuously with 0.1C (Fig. 3).

$$R_{dis} = (OCV - V)/I_{dis} \tag{3}$$

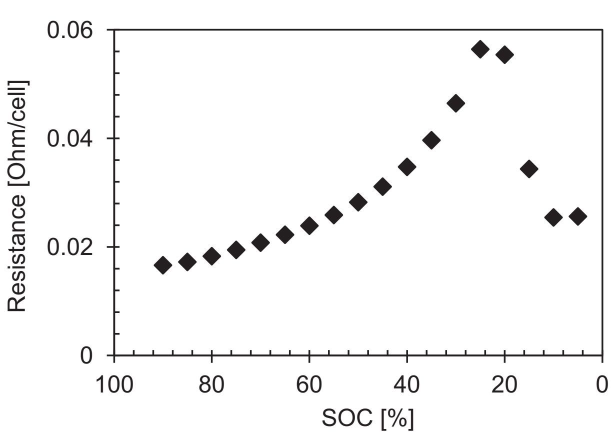

Fig. 3. Resistance while discharging with 0.1C at 240 °C.

where OCV is the measured open-circuit voltage after discharging, V the measured battery voltage and I_{dis} the discharge current.

Between 20% and 25% SOC the Fe-reaction starts next to the solid electrolyte and the smaller resistance of the Fe-cell reduces the total cell resistance even though the DOD (depth-of-discharge) increases further.

3.2. Temperature dependence of the discharged energy

The energy delivered from the battery at 240 °C, 275 °C and 310 °C initial temperature while discharging from 100% to 20% SOC is shown in Table 2. The temperature remains constant during the discharge with 0.1C but increases at higher discharge rates. This rise of temperature is more pronounced when the initial temperature is lower due to the higher internal resistance and the smaller heat transfer losses. The difference in the total discharged energy between 0.25C and 0.1C ranges from 131 to 160 Wh with the biggest deviation occurring at 240 °C. The reason for this is the larger temperature increase at 0.25C and 0.175C when the initial temperature is 240 °C instead of 275 °C or 310 °C which leads to a bigger decrease in the internal resistance and thus to more significant improvement in the discharged energy from lower to higher discharge rates. Moreover, the conductivity of beta-alumina electrolyte and thus the internal resistance, show a non-linear dependency on the temperature.

When the temperature remains constant, as in case of the discharge with 0.1C, 33 Wh less energy is discharged at 240 °C compared to 310 °C. This energy is released as additional Joule heat in the battery's internal resistance. The maximum reduction of the discharged energy when discharging with the same C-rate from 240 °C initial temperature instead of 275 °C or 310 °C is 62 Wh. This energy loss is however much lower than the measured decrease in the discharged energy when the discharge current increases from 0.1C to 0.25C at the usual operating temperatures.

3.3. Capacity measurements

The available total capacity of one battery string was measured at 240 °C, 275 °C and at 310 °C (Fig. 4) after fully charging one of the two parallel strings and then discharging until the end-of-discharge voltage of 41 V was reached. With 0.1C constant discharge current the total capacity is 42.7 Ah/string at 240 °C and 43.6 Ah/string at 275 °C and 310 °C respectively. Compared to the usual operating temperature 1.8% capacity loss occurs when the battery is operated at 240 °C. At higher current (0.25C) 3.3% reduction in the total capacity was measured when the initial operating temperature was 240 °C. During the capacity measurement with 0.25C the temperature increases by 23 °C and 15 °C when the initial temperature is 240 °C and 275 °C respectively. This temperature increase is however lower than it would have been if

Table 2
Discharged energy and measured temperature rise while discharging from 100% to 20% SOC with 0.1C–0.25C at 240 °C, 275 °C and 310 °C initial operating temperature.

Initial temperature [°C]	Discharge current [C-rate]	Discharged energy [kWh]	Temperature increase [°C]
240	0.1C	3.17	0
	0.175C	3.09	18
	0.25C	3.01	37
275	0.1C	3.18	0
	0.175C	3.11	11
	0.25C	3.04	28
310	0.1C	3.20	0
	0.175C	3.12	4
	0.25C	3.07	19

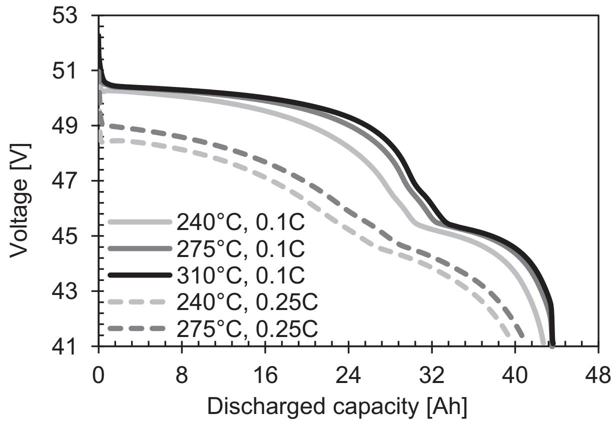

Fig. 4. Measurement of the total available capacity of one battery string at 240 °C, 275 °C and 310° initial temperature.

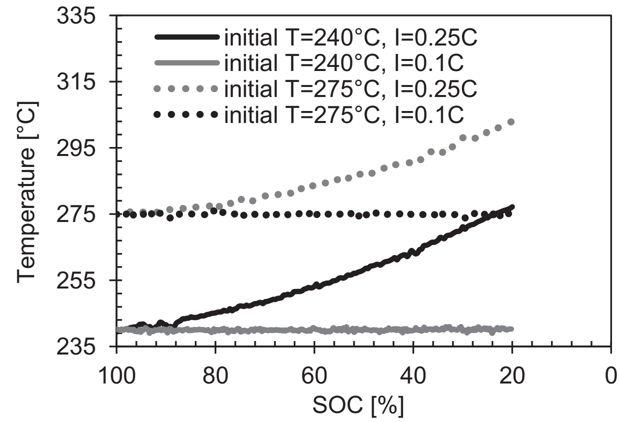

Fig. 5. Evolution of temperature while discharging with 0.1C, 0.25C from 100% to 20% SOC when the initial operating temperature is 240 °C or 275 °C.

both strings were discharging with 0.25C or if the battery had better thermal insulation. Therefore, the total available capacity at this discharge rate may differ slightly depending on the battery's design and size.

3.4. Heating demand and temperature progression while discharging

The change in the internal temperature of a sodium metal chloride battery is given by Eq. (4)

$$\Delta T_{\text{battery}} = (\Delta Q_{\text{joule}} + \Delta Q_{\text{heating}} + \Delta Q_{\text{reversible}} + \Delta Q_{\text{heat loss}})/(m * C) \quad (4)$$

where T_{battery} is the temperature of the battery, Q_{joule} the irreversible heating energy due to losses in the internal resistance, $Q_{\text{reversible}}$ the reversible heat losses, which are positive when discharging and negative when charging, $Q_{\text{heat\_loss}}$, the heat dissipation due to heat transfer processes, Q_{heating} the heating energy provided externally, m the battery's weight and C the thermal capacity of the battery which increases with increasing SOC and temperature [13].

The heat transfer losses equal the externally required heating energy for keeping the temperature constant when the battery is in stand-by mode and they are almost a linear function of the temperature (Table 3).

The battery's temperature and the evolution of the heating demand while discharging with 0.25C and 0.1C when the initial operating temperature is 240 °C and 275 °C are shown in Figs. 5 and 6. At 0.25C discharge current the heating demand drops to zero before 5% DOD is reached. During the discharge with 0.1C the temperature remains constant but the required heating power decreases continuously due to the increasing internal heat generation as the resistance is rising. At 240 °C no externally provided heating energy is needed any more from 26% until 20% SOC. At this

Table 3
Heating demand for compensating the heat transfer losses and keeping the temperature of the 80 Ah battery constant in stand-by mode. The room temperature was 21 °C.

Battery temperature [°C]	Heating demand in stand-by mode [W]
240 °C	48
260 °C	54
275 °C	58
310 °C	67

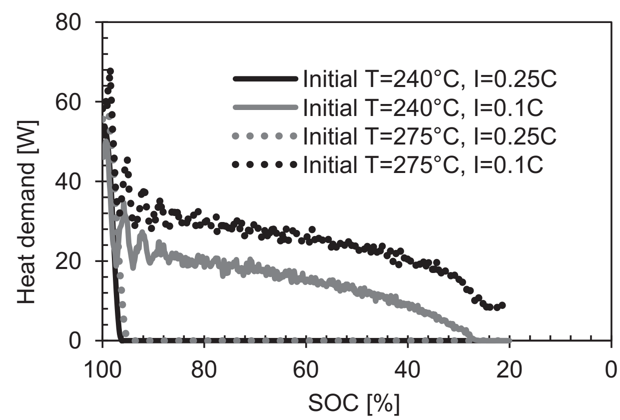

Fig. 6. Required heating power while discharging with 0.1C, 0.25C from 100% to 20% SOC.

point the heat dissipation must be equal to the sum of the reversible and irreversible heat. At 275 °C a stabilization of the heating demand is observed towards the end of the discharge. Since the OCV of the Fe-cell is reached when the SOC is 24% the reason for this is most likely the reduction of the internal heat generation due to the decrease of the internal resistance.

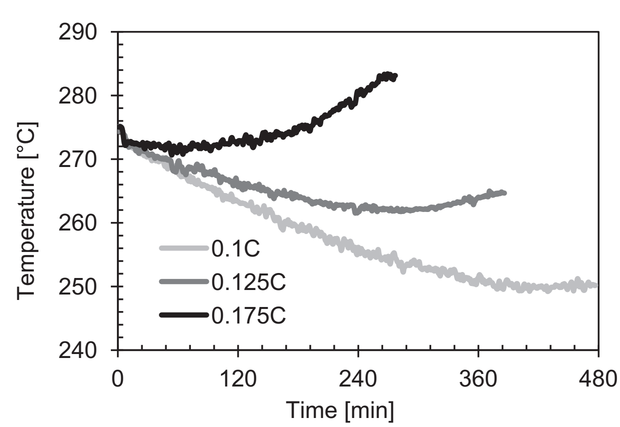

Fig. 7. Temperature development when no external heating energy is provided during the battery's discharge from 100% SOC until 20% SOC with three different currents at 275 °C initial operating temperature.

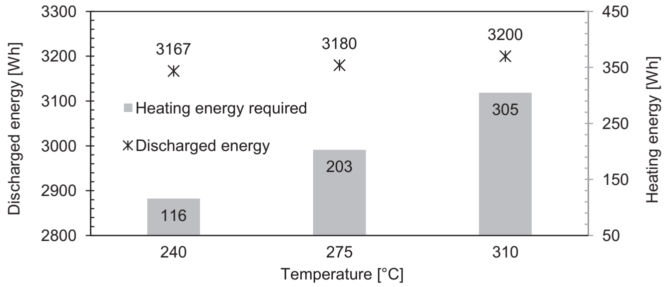

Fig. 8. Required heating energy and discharged energy from 100% to 20% SOC with 0.1C at 240 °C, 275 °C and 310 °C.

If the externally provided heating is switched off while discharging from 100% to 20% SOC with 0.1C, 0.125C or 0.175C the temperature development until the end of the discharge is shown in Fig. 7.

At the beginning of the discharge with 0.1C the battery's temperature decreases since the heat transfer losses exceed the generated Joule heat in the internal resistance and the reversible heat released due to the chemical reactions. As the battery temperature drops the heat dissipation decreases. At the same time the internal resistance increases as the reaction front moves deeper in the cathode and when the temperature is 250 °C the rate of internal heat generation becomes equal to the rate of heat dissipation and the temperature stabilizes at this level for 1 h until the end of the measurement. At 0.125C the reversible and irreversible heat generation leads to a slight temperature rise up to 265 °C after the minimum temperature of 262 °C is reached. Finally with 0.175C discharge current almost no heating energy is required. The lowest temperature (271 °C) is measured after 1 h before the temperature starts increasing until a maximum of 283 °C is recorded at 20% SOC.

In order to evaluate the performance of the sodium metal chloride battery at lower temperatures, the overall efficiency including the thermal losses, should be considered and compared to the normal operating temperatures. The discharged energy and the externally provided heating energy were recorded while discharging the 80 Ah battery with 0.1C from 100% SOC until 20% SOC at three different temperatures (Fig. 8). It is shown that a decrease in the operating temperature from 275 °C to 240 °C results in 43% reduction in the required heating energy whereas the discharged energy is reduced by less than 1%. It can be concluded, that the energy delivered to the load, calculated by subtracting the heating energy from the discharged energy, is maximized at 240 °C.

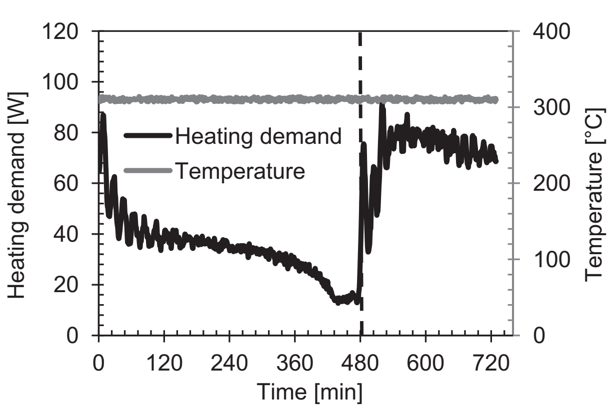

Fig. 9. Evolution of the heating demand and of the temperature during the discharge with 0.1C at 310 °C and after the end of discharge (shown with dashed line) until the heating demand returns to the expected level in stand-by mode.

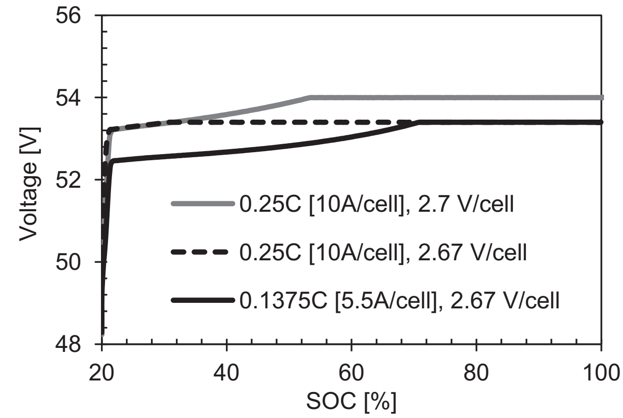

Fig. 10. Voltage development while charging at 310 °C from 20% SOC with three different IU-charge regimes until the end-of-charge criterion is met.

After a discharge the heating demand does not return immediately to the expected level measured in stand-by mode. The end of a discharge at 310 °C is shown in Fig. 9 with dashed line. It can be seen that the heating demand is lower than in stand-by mode almost 1 h after the discharge is ended even though there is no internal heat generation. During that time the recorded temperature remains however constant at 310 °C. This is most likely due to the position of the temperature sensor in the middle of the battery case. The sensor does not detect immediately the temperature drop of the outer cells, which start cooling down after the battery's discharge has been completed.

3.5. Temperature dependence of charging with different charging regimes

The influence of the charging regime and the temperature on the charging process were examined. The duration of the CC phase of the charge depends on the maximum charging voltage, the temperature and the position of the reaction front [10]. In order to ensure that the reaction front will follow the same path during all measurements, the battery was fully charged and then discharged continuously until 20% SOC was reached. Then we applied the charging regime under examination until the end-of-charge criterion was met. This criterion was a charge acceptance smaller than 1.25 mA Ah^{-1} for at least 0.5 h. In Fig. 10 the progression of the voltage while charging at 310 °C constant temperature can be seen. The duration of charge at 275 °C and 310 °C when different charging regimes are applied is shown in Table 4.

In the 48TL80 battery a IU-charge with 5.5 A/cell (0.1375C), 2.67 V/cell is used. Increasing the charging current by 82% from 5.5 A/cell to 10 A/cell (0.25C), while keeping the charging voltage constant at 2.67 V/cell has only a small impact in the duration of charging at 275 °C since when applying the 10 A/cell charging current from 20% SOC the voltage limit is reached in the first 5 min, when the SOC is 22%. Equivalently the CC phase at 310 °C is ended

Table 4
Duration of charging from 20% SOC until the charge acceptance remained below 1.25 mA Ah^{-1} for 0.5 h. Three different charging regimes at 275 °C and 310 °C were tested.

Applied charging voltage, current [V/cell, C-rate]	Duration of charging at 275 °C [h]	Duration of charging at 310 °C [h]
2.67, 0.1375C	10.85	9.3
2.67, 0.25C	10.28	8.1
2.7, 0.25C	8.1	6.75

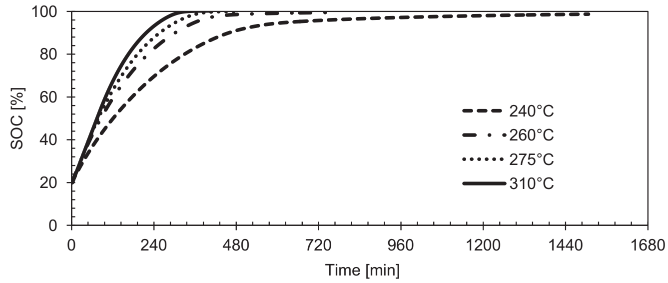

Fig. 11. Duration of charging from 20% SOC while applying the quickest IU-charge (0.25C, 2.7 V/cell) at 240 °C, 260 °C, 275 °C and 310 °C.

when the SOC is 30%, however the current does not drop as quickly as at 275 °C during the CV phase, thus the battery's charge lasts 2.2 h less (Table 4).

A much smaller increase of the charging voltage by 1.1% from 2.67 V/cell to 2.7 V/cell reduces the charging time by at least 2.2 h in the examined temperature window. At 310 °C the CC phase with 0.25C current is prolonged until 53% SOC is reached whereas at 275 °C the maximum charging current can be applied ~30 min longer. However, the higher charging voltage increases the required charging energy from 20% SOC by ~50 Wh to 3453 Wh (at 275 °C).

From these results a significant influence of temperature on the speed of charging due to the decrease of the battery's resistance at higher temperatures was identified. At 275 °C, the battery's charging lasts 1.35–2.2 h longer than at 310 °C when using the same charging regime.

The quickest charging process (0.25C, 2.7 V/cell) was also applied at 240 °C and 260 °C. In Figs. 11 and 12 the increase of the SOC and the decreasing charge acceptance at 240 °C, 260 °C, 275 °C and 310 °C are shown respectively. The temperature remained always constant while charging.

Charging at 240 °C from 20% until the end-of-charge criterion is met lasts 25 h. At the end of charging the charge acceptance is 1.11 mA Ah^{-1}, the charged energy 3.40 Wh and the SOC 98.7%. In comparison, the equivalent measurement at 260 °C is terminated after 13.3 h at 99.6% SOC while the charging current is 0.99 mA Ah^{-1}and the charged energy 3.43 Wh. The duration of charge is thus two times longer at 260 °C than at 310 °C.

If shorter charging time is required for a specific application the battery could be heated for charging and left to cool down while discharging. Otherwise it could be operated from 20% to 90% SOC or from 20% to 80% which would result in much shorter charge durations as shown in Table 5.

Table 5
Duration of charging and required energy for charging and heating for a limited SOC-window.

Temperature [°C]	SOC-operation window	Duration of charging [h]	Charged energy [kWh]	Heating demand while charging [kWh]
240	20%–80%	5.5	2.59	0.28
	20%–90%	7.6	3.02	0.39
260	20%–80%	3.7	2.59	0.22
	20%–90%	5.0	3.02	0.30
275	20%–80%	3.2	2.59	0.20
	20%–90%	4.3	3.02	0.27

From Tables 3 and 5 it can be concluded that the heating energy when charging is in total 14–30 Wh higher than the energy that would have been required for keeping the temperature stable if the battery was inactive during the same time. That means that the endothermic charge reaction, $Q_{reversible}$, absorbs while charging more energy than the total energy released due to the losses in the internal resistance, Q_{joule}. The progression of the heating demand while charging at 260 °C and 310 °C is shown in Fig. 13. At the beginning of the charge when the charging current is high more reversible heat is absorbed and since the internal resistance is still low an increase in the heating demand is observed. Towards the end of the charge the reaction takes place so slowly that the reversible heat is compensated by the losses in the internal resistance resulting in a heating demand which is equal to the heat transfer losses. The maximum heating demand while charging with the quickest regime is 13 W and 7 W higher at 310 °C and 260 °C respectively than the stand-by heating demand. The bigger deviation at 310 °C is caused by the higher charge acceptance and the lower internal resistance compared to the lower operating temperature.

3.6. Total battery efficiency during cycling

The heating demand of a sodium metal chloride battery depends on the battery's design and size but also on the battery's use. Therefore the total battery efficiency while varying the frequency of cycling was calculated. Three different discharge currents were applied. The used charging regime was the quickest IU-charge examined here with 0.25C charging current and 2.7 V/cell charging voltage until the end-of-charge criterion was fulfilled (1.25 mA Ah^{-1} for at least 0.5 h). The battery was fully charged and subsequently discharged with 0.1C until 90% SOC was reached.

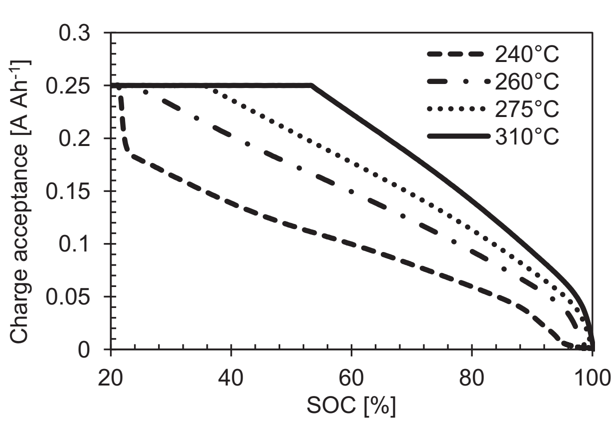

Fig. 12. Charge acceptance while charging with 0.25C (10 A/cell), 2.7 V/cell from 20% SOC until the end-of-charge criterion is met.

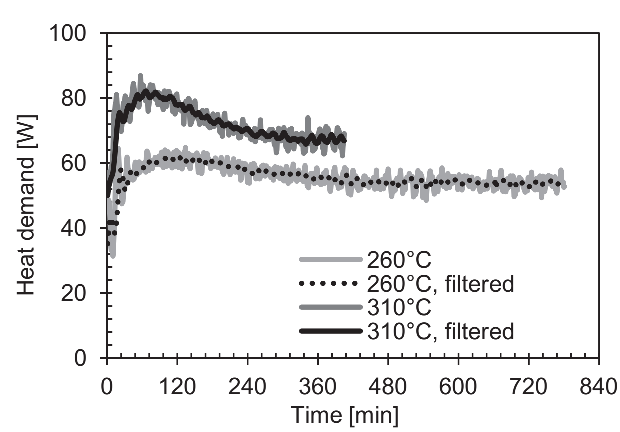

Fig. 13. Heating demand while charging with 0.25C (10 A/cell), 2.7 V/cell from 20% SOC at 260 °C and 310 °C. A moving average filter was applied for smoothing out the short-term fluctuations.

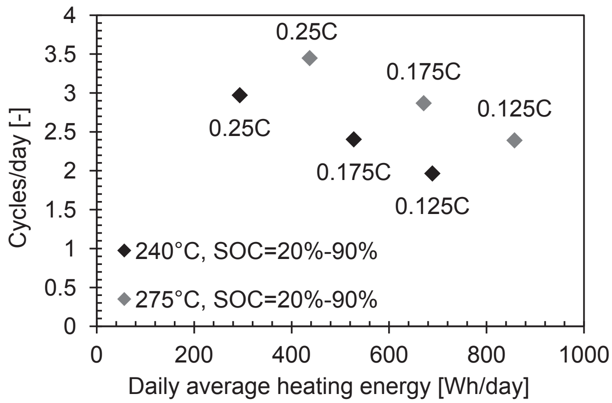

Fig. 14. Daily heating demand and maximum number of cycles if the battery is discharged with 0.125C–0.25C current and charged with 0.25C, 2.7 V/cell in a SOC-window from 20% to 90% at 240 °C and 275 °C initial operating temperature.

Then two discharge–charge cycles were performed in the SOC-window 90%–20% with 30 min pause in-between. The measured parameters of the second cycle were used for the calculations.

The maximum number of cycles that can be delivered daily by the tested sodium metal chloride battery when the initial operating temperature is 240 °C or 275 °C and for 0.125C–0.25C constant discharge current is shown in Fig. 14. The daily average heating energy if the battery is continuously cycled, also shown in Fig. 14, is the product of the required heating energy for one cycle and of the maximum number of cycles per day. If the battery is cycled with the same parameters at 240 °C ~0.5 cycles less can be performed on a daily basis compared to 275 °C due to the slower charging. In exchange to this lower utilization, 140–170 Wh less heating energy is required on average and in a daily basis at 240 °C compared to 275 °C when the battery is cycled with the same discharge current.

The efficiency of a single cycle, $\eta_{\text{per-cycle}}$, is shown in Table 6. It is defined as:

$$\eta_{\text{per-cycle}} = \frac{E_{\text{discharge}}}{E_{\text{charge}} + E_{\text{heating}}} \tag{5}$$

where $E_{\text{discharge}}$ is the discharged energy, E_{charge} the charged energy and E_{heating} the additionally required heating energy during that cycle.

Even though the heating demand at 240 °C is lower due to the lower operating temperature the longer duration of charging results in almost the same total required heating energy as at 275 °C. Except for this, ~25 Wh more energy is discharged per cycle at 275 °C compared to 240 °C. Thus the cycle efficiency at 275 °C is slightly better or the same, depending on the discharge current. The maximum cycle efficiency reached with the tested battery was 85% with 0.25C discharge current.

If the battery is not cycled continuously, which is the case in most of the applications, the cycle efficiency is not representative of the battery's efficiency because heating energy has to be provided additionally when the battery is not operated for maintaining the temperature constant. Therefore the daily efficiency, η_{daily}, given by Eq. (6), is introduced:

$$\eta_{\text{daily}} = \frac{E_{\text{discharge}}}{E_{\text{charge}} + E_{\text{heating}} + \left(24 - t_{\text{cycle}}\right) * P_{\text{stand-by}}} \tag{6}$$

where t_{cycle} the duration of the cycles in hours and $P_{\text{stand-by}}$ the heating demand when the battery is in stand-by mode (Table 3). The calculation of the daily efficiency from the equation above is based on the condition that the initial operating temperature is reached again before the end of the cycle. This was always the case even with the highest discharge currents (0.25C).

Table 6 shows the calculated daily efficiencies for different cycling frequencies. The efficiencies are not given if the relevant cycling frequency cannot be achieved in a day with the specified discharge rate. However when the initial temperature is 240 °C and the battery performs 3 cycles/day with 0.25C discharge current the total duration is 24.2 h. In that case there is no stand-by time. Therefore the daily efficiency is equal to the cycle efficiency, i.e. 85%.

Generally, the daily efficiency is higher at lower temperatures since in stand-by mode the heating demand is 48 W at 240 °C whereas at 275 °C 58 W are required for keeping the temperature stable. When the battery is cycled at 240 °C, the percentage of discharged energy used for heating is reduced by 21%–48% in the 20%–90% SOC-window. As a result, the daily efficiency at 240 °C is 1%–6% higher compared to 275 °C for the same cycling frequency and discharge rate. The efficiencies presented here are expected to be higher for batteries with lower surface to volume ratio and for batteries with vacuum insulation. This type of insulation is commercially available and reduces the thermal conductivity by more than 50%.

4. Conclusions

The main objective of the present study was to test the performance of a 80 Ah sodium metal chloride battery with commercially available tubular cells (MLX-3 type) at temperatures lower than the usual operating temperatures of this technology, which would allow a reduction of the battery's heat demand. It was shown that the operation at temperatures as low as 240 °C is not only feasible but also advantageous for the overall system efficiency. The total available capacity measured with 0.1C current was found to be only 1.8% lower at 240 °C constant temperature compared to the normal operating conditions, at 275 °C and 310 °C. When discharging with the same current 80% of the nominal capacity until 20% SOC the energy delivered to the load after subtracting the required heating energy is maximized at 240 °C. The energy gain when operating the

Table 6
Cycle efficiency and daily battery efficiency depending on the cycling frequency when the battery is operated in a SOC-window from 20% to 90% with 0.125C–0.25C constant discharge current.

Initial temperature [°C]	SOC-operation window	Current during discharge	Total battery efficiency/cycle $\eta_{\text{per-cycle}}$ [%]	Total battery efficiency/day η_{daily} [%]		
				Cycling frequency		
				1 cycle	2 cycles	3 cycles
240	20%–90%	0.125C	81%	70%	–	–
		0.175C	83%	69%	81%	
		0.25C	85%	68%	80%	85%
275		0.125C	82%	66%	79%	–
		0.175C	84%	66%	79%	–
		0.25C	85%	65%	78%	84%

sodium metal chloride battery at lower temperatures derives from the reduced heat transfer losses, which were 48 W at 240 °C, 10 W lower than at 275 °C.

However, at 240 °C with the quickest IU-charge (2.7 V/cell, 10 A/cell) around 25 h charging time was required from 20% SOC until the end-of-charge criterion was met. For a SOC increase from 20% to 90% at 240 °C the duration of charging is reduced to 7.6 h. At this SOC-window the total daily efficiency is always higher at 240 °C when the discharge current ranges from 0.125C until 0.25C even though the cycle efficiency is slightly lower or the same at 240 °C compared to 275 °C. The reason for the improvement of the total battery efficiency at 240 °C are the lower heat transfer losses which result in up to 49% reduction in the percentage of the discharged energy that is used as heating energy at the same cycling frequency.

References

[1] J. Kummer, Prog. Solid State Chem. (1972) 141–175.
[2] J.L. Sudworth, J. Power Sources 100 (2001) 149–163.
[3] C.H. Dustmann, J. Power Sources 127 (2004) 85–92.
[4] J.L. Sudworth, J. Power Sources 51 (1994) 105–114.
[5] J.L. Sudworth, R.C. Galloway, in: J. Garche (Ed.), Encyclopedia of Electrochemical Power Sources, Elsevier Ltd, Oxford, 2009, pp. 312–333.
[6] L. Gaillac, D. Skaggs, N. Pinsky, in: 28th Annual International Telecommunications Energy Conference (INTELEC), Providence, 10–14 September 2006.
[7] J. Rijssenbeek, H. Wiegman, D. Hall, C. Chuah, G. Balasubramanian, C. Brady, in: 33rd International Telecommunications Energy Conference (INTELEC), Amsterdam, 09–13 October, 2011.
[8] D.J.L. Brett, P. Aguiar, N.P. Brandon, R.N. Bull, R.C. Galloway, G.W. Hayes, K. Lillie, C. Mellors, C. Smith, A.R. Tilley, J. Power Sources 157 (2006) 782–798.
[9] J. Dixon, I. Nakashima, E.F. Arcos, M. Ortuzar, IEEE Trans. Ind. Electron. 57 (2009) 943–949.
[10] T.M.O. Sullivan, C.M. Bingham, R.E. Clark, in: International Symposium on Power Electronics, Electric Drives, Automation and Motion, Taormina, 23–26 May 2006.
[11] X. Lu, G. Li, J.Y. Kim, J.P. Lemmon, V.L. Sprenkle, Z. Yang, J. Power Sources 215 (2012) 288–295.
[12] M. Hosseinifar, A. Petric, J. Power Sources 206 (2012) 402–408.
[13] B. Cleaver, D.J. Cleaver, L. Littlewood, D.S. Demott, J. Appl. Electrochem. 25 (1995) 1128–1132.

Glossary

SOC: state-of-charge
OCV: open-circuit voltage
DOD: depth of discharge
BMS: battery management system
$E_{discharge}$: discharged energy
E_{charge}: charged energy
$E_{heating}$: required heating energy
$P_{stand\text{-}by}$: heating demand in stand-by mode